Picosecond Time-Resolved Raman Study of *trans*-Azobenzene

Tatsuya Fujino and Tahei Tahara*

Institute for Molecular Science (IMS), Myodaiji, Okazaki 444-8585, Japan

Received: August 5, 1999; In Final Form: October 29, 1999

The electronic and vibrational relaxation of photoexcited *trans*-azobenzene was investigated in solution by picosecond time-resolved Raman spectroscopy. Picosecond time-resolved Raman spectra were measured with the probe wavelength at 410 nm, which is in resonance with a transient absorption appearing after the S_2-($\pi\pi^*$) ← S_0 photoexcitation. Several transient Raman bands assignable to the S_1 state were observed immediately after photoexcitation. The lifetime of the S_1 state showed a significant solvent dependence, and it was determined as ∼12.5 ps in ethylene glycol and ∼1 ps in hexane. Time-resolved anti-Stokes Raman measurements were also carried out for hexane solutions to obtain information about vibrational relaxation process. The anti-Stokes spectra showed that the observed S_1 state was highly vibrationally excited. In addition, several anti-Stokes Raman bands due to the S_0 state were observed after the decay of the S_1 state, indicating that the vibrationally excited S_0 state was generated after electronic relaxation in hexane. The lifetime of vibrationally excited S_0 azobenzene was evaluated as ∼16 ps by the analysis for the intensity change of the anti-Stokes NN stretch band. The assignment of the NN stretch band in the S_1 spectrum was made by using ^{15}N-substituted azobenzene, and it was clarified that the NN stretching frequency in the S_1 state is very close to that of the S_0 state (1428 cm^{-1} in S_1 and 1440 cm^{-1} in S_0). The high NN stretching frequency in the S_1 state indicated that the NN bond retains a double bond nature in the S_1 state. Vibrational assignments for the other S_1 Raman bands were made by one-to-one correspondence between the S_1 and S_0 bands. The double bond nature of the NN bond and the high similarity between the S_1 and the S_0 Raman spectra indicated that the observed S_1 state has a planar structure around the NN bond. The obtained Raman data seemed to suggest that the inversion in the S_1 state takes part also in the isomerization following $S_2(\pi\pi^*)$ photoexcitation. The relaxation process of photoexcited *trans*-azobenzene as well as its photoisomerization mechanism is discussed on the basis of the observed Raman data.

1. Introduction

Azobenzene and its derivatives are prototypical molecules showing cis−trans photoisomerization and are of current interest because of their wide applications such as light-driven switches and image storage devices.[1−3] The properties of azobenzene have been extensively investigated by variety of physicochemical methods including steady-state UV−visible absorption,[4−7] Raman,[8,9] NMR,[10] and theoretical calculations.[11,12] It is now believed that the photoisomerization mechanism of *trans*-azobenzene (we simply call it azobenzene hereafter) strongly depends on the excitation wavelength; with $n\pi^*$ (S_1) excitation the isomerization proceeds with the in-plane inversion at one N atom while under $\pi\pi^*$ (S_2) excitation it takes place by rotation around the N═N double bond. The inversion mechanism was first proposed by Rau and Lüddecke, who observed photoisomerization of azobenzene derivatives in which the rotation was prohibited by chemical modification.[4] On the other hand, it seems that the rotational mechanism has not been fully proved for azobenzene itself, although this mechanism is known as the photoisomerization pathway of olefines.

Time-resolved studies are very important for elucidation of the reaction dynamics of azobenzene. However, the number of the reports is still limited because photoisomerization of azobenzene occurs very rapidly. The first picosecond time-resolved study of azobenzene has been conducted by Struve and Morgante,[13,14] who observed the S_2 and the S_1 fluorescence and evaluated fluorescence lifetime by the Kerr gate method using 8-ps laser pulses. Lednev et al. carried out the first femtosecond UV−visible absorption study and observed transient absorption peaked around 400 nm after the 303-nm excitation to the S_2 state.[15] They measured absorption change at 367, 400, and 420 nm and observed biexpoential decay having time constants of 1 and 15 ps. In the following work undertaken with improved time resolution, they succeeded in observing another transient showing absorption around 475 nm whose lifetime is shorter than 200 fs.[16] In their recent assignment, the 475-nm transient was attributed to the S_2 state of azobenzene that is initially prepared by photoexcitation, and the two components ($\tau_1 \sim$ 1ps, $\tau_2 \sim$ 15 ps) in the transient absorption around 400 nm were ascribed to the "bottleneck" states in the S_2 and S_1 potentials.[16,17] Very similar transient absorptions as well as analogous dynamics were observed for an azobenzene derivative by Azuma et al. although the peak wavelength of the S_2 transient absorption was shifted from ∼475 to ∼490 nm reflecting para substitutions.[18] However, they assigned the second 400-nm transient to the S_1 state of azobenzene. In this sense, the assignment of the 400-nm transient is still unclear. Meanwhile, time-resolved absorption study has been undertaken also for the cis isomer that exists in the photostationary cis/trans balance. It was found that photoisomerization from the cis isomer proceeds with a time constant of ∼170 fs with the excitation at 435 nm.[19] The vibrational cooling process in the electronic ground state has been studied by time-resolved

* To whom correspondence should be addressed.

10.1021/jp992757m CCC: $19.00
Published on Web 01/06/2000

infrared spectroscopy, and it was concluded that the intermolecular energy transfer (energy dissipation) to the solvent takes place on a time scale of ~20 ps.[20]

Thanks to these time-resolved studies, the ultrafast dynamics of photoexcited azobenzene has been clarified to some extent. However, the assignment of each dynamics is still controversial and the structural information about transient species is obviously lacking. Time-resolved resonance Raman spectroscopy is a very powerful tool to study photochemical reactions, and it often affords unique information that cannot be obtained by other spectroscopy: Raman spectra contain much information about molecular structure of transient species, and anti-Stokes measurements give clear information about vibrational relaxation process. Therefore, it is highly desirable to apply Raman spectroscopy to the study of ultrafast dynamics of azobenzene. In general, vibrational spectroscopy requires high-frequency resolution compared with electronic spectroscopy such as UV−visible absorption. For the molecules in solution, the frequency resolution as high as 10 cm^{-1} is needed to obtain well-resolved vibrational spectra. This fact practically limits the upper time resolution of Raman measurements to about 1 ps. From this viewpoint, azobenzene that shows very fast dynamics is one of the most challenging targets for time-resolved Raman spectroscopy. In this paper, we report our picosecond time-resolved resonance Raman study of *trans*-azobenzene. We present Raman spectra of the 400-nm transient, which we assign to the S_1 state of azobenzene. The NN stretch frequency in the S_1 state is determined by ^{15}N substitution, and the molecular structure of the S_1 state is discussed. Raman scattering from the vibrationally hot ground state is also observed, and the relaxation dynamics including vibrational cooling process is clarified.

2. Experimental Section

The experimental setup used for picosecond time-resolved Raman measurements is described in detail elsewhere.[21] Briefly, a mode-locked Ti:sapphire laser (Spectra-Physics, Tsunami) that was pumped by an Ar^+ laser (Spectra-Physics, Beam lok 2060-10SA) provided picosecond pulses (820 nm, 13 nJ, 1.8 ps) at a repetition rate of 90 MHz. The output from the Ti:sapphire oscillator laser was amplified up to an energy of ~1 mJ with a regenerative amplifier (Spectra-Physics, Spitfire, 1 kHz) that was pumped by a CW Q-switched Nd:YLF laser (Spectra-Physics, Merlin). The amplified pulses were frequency doubled by a 5-mm LBO crystal (410 nm, 120 μJ) and then tripled by a 5-mm BBO crystal (273 nm, 110 μJ). The generated second and third harmonic pulses were used as the probe and the pump pulses, respectively, in the time-resolved measurements. The pump and probe pulses were separated by a dichroic mirror and were introduced to different variable delay lines to make a time delay. Then the two beams were recombined and focused onto a thin-film-like jet stream of the sample solution with a quartz lens (f = 50 mm). The intensity of the probe pulse passing through the sample was monitored by a photodiode with a boxcar averager (Stanford Research System, SR 250) in order to check the spatial/temporal overlap of the pump and probe pulses by measuring transient absorption at the probing wavelength. Typical energy of the pump and probe pulses were ~20 and 3−10 μJ at the sample position, respectively. Raman scattering from the sample were analyzed with a polychromator (Jovin-Yvon, HR-320) and detected by a liquid-nitrogen-cooled CCD detector (Princeton Instruments, LN/CCD-1100PB). The frequency resolution was about 11 cm^{-1}, which was determined as the full spectral width at half-maximum of the Rayleigh scattering. In this setup, a mirror can be inserted before the sample position in order to introduce the pump and probe beams to an optical setup for Kerr effect measurements. The delay time origin (t_d = 0 ps) as well as the time resolution of the measurements was checked by measuring the Kerr effect of heptane. A typical time resolution was evaluated as about 2.8 ps. In all Raman measurements, the polarization of pump and probe pulses were set parallel with the intention of getting larger transient signals especially in early delay time. Under this condition, the temporal change of transient Raman signals (and the evaluated decay time constants) are affected by the rotational diffusion of the molecule to some extent. However, the effect of rotational diffusion was not sizable as checked by transient absorption polarization measurements, and it does not influence any arguments in this paper. All measurements were performed at room temperature.

Azobenzene (trans) was purchased from Wako Pure Chemical Industries and was recrystallized two times from methanol. ^{15}N-substituted azobenzene, $(C_6H_6{}^{15}N)_2$, was synthesized and purified according to the literature.[22] Both samples, normal and isotopic substituted azobenzene, were sufficiently dried in a drybox before use. The samples were dissolved in hexane (Wako Pure Chemical Industries, special grade) or in ethylene glycol (Wako Pure Chemical Industries, special grade), and the solutions with the concentration of 1.5×10^{-2} mol dm^{-3} were used for the Raman experiments. A fresh sample solution was prepared and used in the dark for each time-resolved measurement. The amount of the cis isomer in the solution, which was produced by photoisomerization, was negligibly small because the cis isomer thermally returns to the trans form with a time constant as short as ~50 μs.[23]

3. Results and Discussion

3.1. Time-Resolved Raman Spectra in Ethylene Glycol: Observation of the S_1 State. In the UV−visible region, ground-state azobenzene exhibits two absorption bands around ~310 and ~450 nm, and those bands have been assigned to the S_2 ($\pi\pi^*$) ← S_0 and the S_1 ($n\pi^*$) ← S_0 transitions, respectively. The pumping wavelength (273 nm) in the present experiments corresponds to the blue side of the S_2 ← S_0 absorption ($\epsilon_{273} \approx$ 6100 mol^{-1} dm^3 cm^{-1}), and the molecule is initially excited to the S_2 ($\pi\pi^*$) state under this photoexcitation condition. The probe wavelength (410 nm) is in resonance with the absorption of the 400-nm transient that appears in accordance with the decay of the S_2 state when the molecule is photoexcited to the S_2 state. It was reported for an azobenzene derivative that the lifetime of the 400-nm transient strongly depends on the solvent viscosity: it changes from ~1 ps in hexane to ~10 ps in highly viscous ethylene glycol.[18] We measured transient absorption at 410 nm for azobenzene itself and confirmed that the lifetime of the transient becomes as long as 11 ps in ethylene glycol. Because of this much longer lifetime of the transient, we first carried out time-resolved Raman measurements in ethylene glycol.

Figure 1 shows picosecond time-resolved Raman spectra obtained from ethylene glycol solution at the delay time of 0 ps. In the spectrum taken with the pump and probe irradiation (Figure 1a), Raman scattering was observed on the high luminescence background that presumably arises from the S_2 fluorescence of azobenzene. We subtracted fluorescence background from the spectrum by using the fluorescence spectrum measured with the only pump irradiation (Figure 1b), and the resultant subtracted spectrum is shown in Figure 1c. All the prominent Raman bands observed in this spectrum are the Raman bands of S_0 azobenzene or solvent, and it was a little

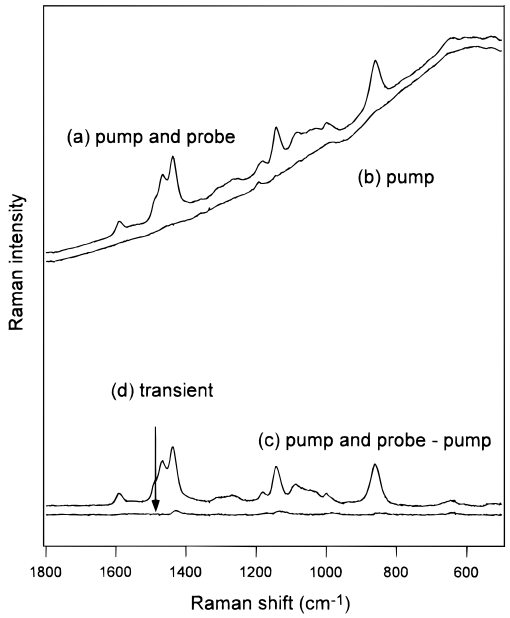

Figure 1. Picosecond time-resolved Raman spectra of *trans*-azobenzene in ethylene glycol at the delay time of 0 ps (1.5×10^{-2} mol dm^{-3}; pump laser 273 nm; probe laser 410 nm): (a) Raman spectrum obtained with pump and probe irradiation; (b) Raman spectrum obtained with pump; (c) subtracted spectrum, (a) − (b). Subtraction of the Raman bands of S_0 azobenzene and ethylene glycol from the spectrum c gave the transient Raman spectrum shown in (d).

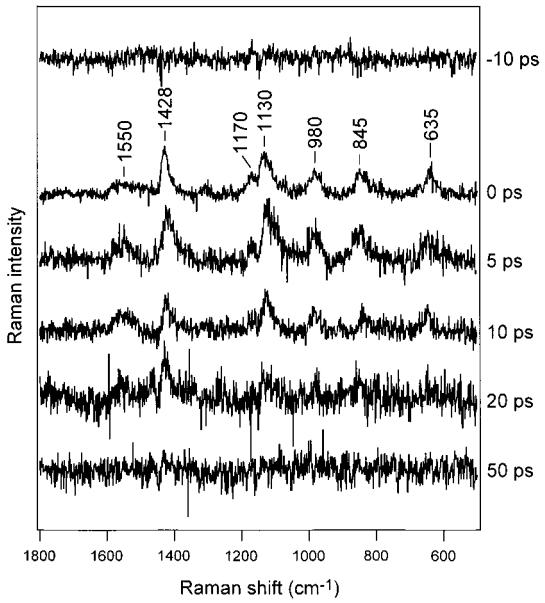

Figure 2. Picosecond time-resolved Raman spectra of *trans*-azobenzene in ethylene glycol in the delay time range from −10 to 50 ps (1.5×10^{-2} mol dm^{-3}; pump laser 273 nm; probe laser 410 nm). The Raman intensity at each delay time has been normalized by using the solvent band intensity.

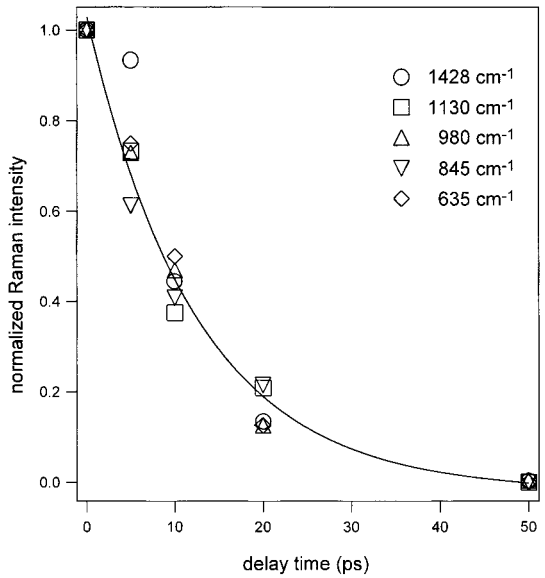

Figure 3. Intensity changes of transient Raman bands in ethylene glycol. The solid line is the best fitted single-exponential function having a time constant of 12.5 ps. The intensity of each band was normalized to unity at 0 ps.

difficult to recognize the Raman signal arising from the transient species. However, when we carefully subtract Raman bands of S_0 azobenzene and solvent from the spectrum, we were able to see very weak but clear Raman signals ascribable to the transient species, as shown in Figure 1d. Under the present experimental condition, we needed a careful subtraction procedure to make the transient Raman bands noticeable. It is not only due to the weakness of the transient Raman bands but also owing to the high Raman intensity of S_0 azobenzene. The Raman intensity of S_0 azobenzene is highly enhanced under the present probing condition thanks to the resonance effect originating from the $n\pi^*$ transition and/or preresonance effect due to the $\pi\pi^*$ transition. The resonantly enhanced strong S_0 Raman bands mask transient Raman signals. Time-resolved Raman spectra shown in this paper hereafter have been obtained after subtracting S_0 and solvent Raman bands as well as fluorescence background.

Figure 2 depicts picosecond time-resolved Raman spectra of ethylene glycol solution in the delay time range from −10 to 50 ps. The Raman intensity at each delay time has been normalized by using intensity of the solvent Raman bands. (Note that the solvent Raman bands were already subtracted and hence are not shown in the spectra.) Immediately after photoexcitaion, we observed prominent transient Raman bands at 1428, 1130, 980, 845, and 635 cm^{-1} as well as weak ones at ∼1550 and 1170 cm^{-1}. These bands disappeared with increasing delay time and completely vanished after 50 ps. The temporal changes of the normalized intensity of the five transient Raman bands are plotted in Figure 3. The decays of the observed transient Raman bands were indistinguishable within experimental error, and they were well fitted by a single-exponential function having a lifetime of ∼12.5 ps (the solid curve in the figure). The obtained lifetime of the transient Raman bands is in good agreement with the lifetime of the 400-nm transient in ethylene glycol. The identical decay of all the transient Raman bands indicated that these bands are ascribed to a single transient species. Judging from its lifetime of ∼10 ps, the observed transient, i.e., the 400-nm transient in ethylene glycol, is safely assigned to the S_1 state of azobenzene.

It should be mentioned that when we measured time-resolved spectra with the probe pulse whose energy exceeded 10 μJ, several additional transient Raman bands appeared. These Raman bands were observed only in a polar solvent (ethylene glycol) but not observed in a nonpolar solvent (hexane). We tentatively assigned the additional transient Raman bands to the cation of azobenzene that was produced by the multiphoton ionization under the intense laser pulses. It was essential to lower the probe pulse energy down to as low as 3 μJ in order to obtain reliable time-resolved Raman spectra of S_1 azobenzene in ethylene glycol.

It should be also noted that no Raman bands due to the cis isomer were recognized in our time-resolved Raman spectra,

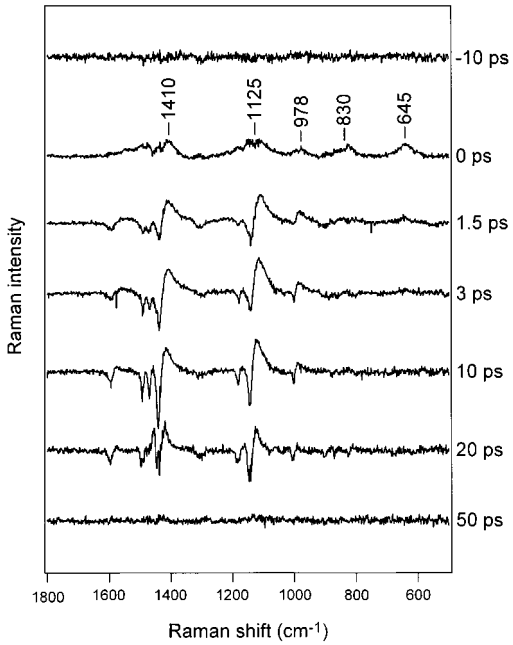

Figure 4. Picosecond time-resolved Raman spectra of *trans*-azobenzene in hexane in the delay time range from −10 to 50 ps (1.5×10^{-2} mol dm^{-3}; pump laser 273 nm; probe laser 410 nm). The Raman intensity at each delay time has been normalized by using the solvent band intensity.

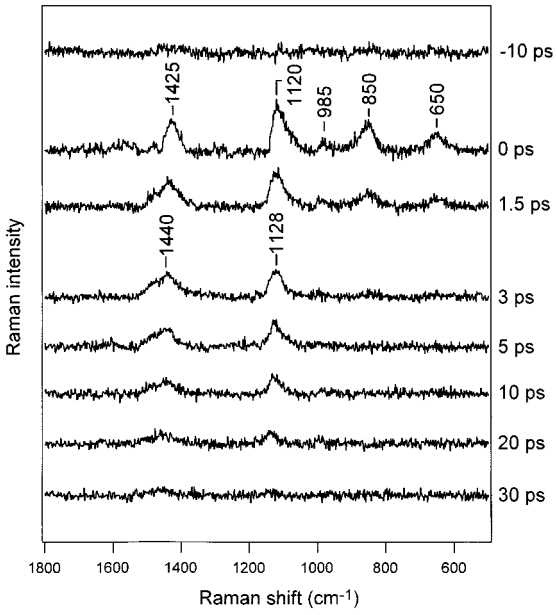

Figure 5. Picosecond time-resolved anti-Stokes Raman spectra of *trans*-azobenzene in hexane in the delay time range from −10 to 30 ps (1.5×10^{-2} mol dm^{-3}; pump laser 273 nm; probe laser 410 nm). The Raman intensity at each delay time has been normalized by using the solvent band intensity.

although the cis isomer is expected to be produced by photoisomerization. The absence of the cis Raman bands is presumably due to the low isomerization quantum yield under S_2 photoexcitation ($\phi = 0.10$)[4] and the small resonance Raman enhancement of the cis isomer at the present probe wavelength.

3.2. Time-Resolved Raman Spectra in Hexane: Observation of the S_1 State and the Vibrationally Excited S_0 State. Next we describe the experimental results obtained from hexane solution. Figure 4 shows picosecond time-resolved Raman spectra of a hexane solution in the delay time range from −10 to 50 ps. The Raman intensity at each delay time has been normalized. As clearly seen, the time-resolved Raman spectra in hexane showed somewhat complicated temporal change. Immediately after photoexcitation, several transient Raman bands were observed. Although some solvent-dependent shifts were recognized, these transient bands were essentially the same as those observed in ethylene glycol solution. Thus, they are ascribable to the S_1 state of azobenzene. These S_1 transient Raman bands disappeared within ∼3 ps in hexane, as most clearly seen for the bands at 830 and 645 cm^{-1}. However, some transient spectral features remained around 1440 and 1140 cm^{-1} where the strong S_0 Raman bands are located. These features changed its shape and became smaller with the increase of the delay time and finally disappeared at 50 ps. The spectral features observed in the region of S_0 Raman bands were not due to artifacts arising from an inadequate subtraction procedure. In fact, we obtained flat subtracted spectra at the negative delay time as well as at 50 ps. The existence of the residual spectral feature around the S_0 Raman band region is reproducible even though some details of the features were affected by small arbitrariness of the subtraction coefficient. The observed Raman spectra indicated that additional dynamics was observed in hexane after relaxation of the S_1 state.

With photoexcitation at 273 nm, the molecule gains the energy greater than 36 000 cm^{-1}. The energy dissipation to the surrounding solvent takes place in a time scale of a few tens of picosecond.[24−26] Therefore, it is expected that a considerable amount of the phoexcitation energy is still localized in an azobenzene molecule even after the $S_1 \rightarrow S_0$ electronic relaxation and that the vibrationally excited ("hot") S_0 state is produced. In general, Raman bands of the vibrationally excited molecule (hot bands) are red-shifted and are broadened compared with those of the "cold" molecules. Thus, we thought that the spectral features in the time region from 1.5 to 20 ps indicated the existence of the vibrationally excited S_0 azobenzene. In other words, they arose from the subtraction of the "cold" S_0 Raman spectrum from the "hot" S_0 Raman spectrum. To verify this argument, we have undertaken picosecond time-resolved measurements of anti-Stokes Raman spectra that directly represent the population of the vibrationally excited state.

Picosecond time-resolved anti-Stokes Raman spectra of azobenzene in hexane are shown in Figure 5. The Raman signals observed only with probe irradiation were already subtracted, and the Raman intensity at each delay time was normalized using the solvent Raman intensity. However, reflecting the small population of the vibrationally excited state in thermal equilibrium, the intensities of the anti-Stokes Raman bands of S_0 azobenzene and solvent were very small compared with those in the Stokes side so that we were able to recognize time-resolved change even without spectrum subtraction. The observed temporal change of the anti-Stokes Raman spectra coincided well with the spectral change observed in Stokes Raman. Immediately after phtoexcitation, the several transient Raman bands assignable to the S_1 state were observed and they disappeared within a few picoseconds. (The frequency difference between the Stokes side and the anti-Stokes side is due to the error in the determination of the peak position.) The intensity pattern of the anti-Stokes S_1 Raman resembled well that of the Stokes Raman, and the high frequency bands appeared with fairly high intensity. This implies that the observed S_1 state is highly vibrationally excited. After the decay of the S_1 state, several anti-Stokes Raman bands remained. The prominent bands are located around ∼1440 and ∼1130 cm^{-1}. Those Raman frequencies are almost identical to the N═N stretch and

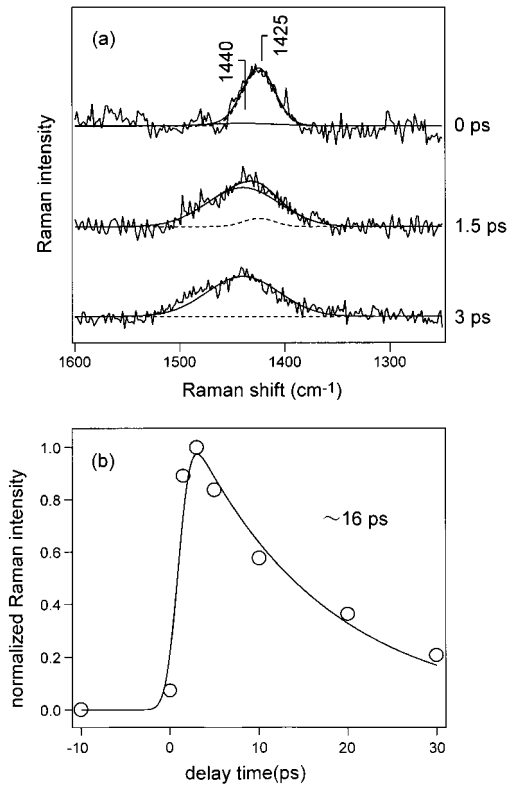

Figure 6. Result of the fitting analysis for the NN stretch region of anti-Stokes Raman spectra in the delay time range from 0 to 3 ps (a). The decomposed bands at 1425 cm^{-1} (S_1; dotted) and 1440 cm^{-1} (S_0; solid) are depicted with thin lines, and the thick lines are the sum. Intensity change of the 1440 cm^{-1} band (b). The solid line is the best-fitted curve having a decay time constant of 16 ps that represents the decay time of vibrationally "hot" S_0 azobenzene. The instrumental response as well as the 1-ps rise is also taken into account.

the C−N stretch bands of S_0 azobenzene,[8,11] respectively, although the observed band shapes were slightly broadened. The intensity of these S_0 anti-Stokes Raman bands decreased within a few tens of picoseconds and returned to the value of thermal equilibrium (zero in the subtracted spectra). The observation in the anti-Stokes side clearly showed that the vibrationally excited S_0 state is generated after the decay of the S_1 state in hexane, which gives rise to the residual features after spectral subtraction in the Stokes Raman spectra.

To obtain more quantitative information about the dynamics in the hexane solution, we carried out a fitting analysis for the anti-Stokes Raman signal in the region around 1400−1500 cm^{-1}. In this analysis, we assumed that the observed Raman feature consists of the S_1 and the S_0 Raman bands having Gaussian band shapes and determined each amplitude with the peak frequencies and the bandwidths fixed. Figure 6a depicts the results of the band decomposition for the delay time range from 0 to 3 ps. The decomposed bands at 1425 (S_1) and 1440 cm^{-1} (S_0) are represented with thin lines, and the thick lines are the sum of them. It is clearly seen that the contribution from the vibrationally excited S_1 azobenzene disappears in a few picoseconds and, in exchange, that of the vibrationally excited S_0 state grows up. We can evaluate the lifetime of the S_1 state to be about ∼1 ps in hexane since the contribution from the S_1 state is completely missing in the Stokes and anti-Stokes Raman spectrum at 3 ps. The lifetime of the vibrationally "hot" S_0 species was evaluated from the time dependence of the 1440-cm^{-1} band intensity. The intensity change of the 1440-cm^{-1} component is plotted in Figure 6b up to 30 ps. The obtained decay was well fitted by an exponential function having a decay time constant of ∼16 ps, which corresponds to the lifetime of the vibrationally excited S_0 species in hexane. The obtained time constant is a typical value for the vibrational cooling time of the photoexcited solute molecule in hydrocarbon.[24−26] This value is also in fairly good agreement with the vibrational cooling time of azobenzene in DMSO-d_6 which was evaluated by femtosecond time-resolved infrared spectroscopy.[20]

It is noteworthy that only the NN stretch and the CN stretch bands were clearly observed for the hot S_0 state in time-resolved anti-Stokes Raman spectra. It suggests that these two vibrational modes are selectively excited with the $S_1 \rightarrow S_0$ electronic relaxation. It should be also noted that the CN stretch band of the hot S_0 state exhibits a significant temporal frequency shift. It is located around ∼1128 cm^{-1} at 3 ps and is shifted to ∼1140 cm^{-1} at 20 ps. The anti-Stokes Raman measurements provide rich and direct information about the vibrational relaxation process of the molecule. The further study of time-resolved anti-Stokes Raman, such as pump wavelength dependence, may shed new light on the understanding of the reaction pathways.

3.3. Vibrational Assignment and Molecular Structure of the S_1 State. In this section, we make vibrational assignments of the observed transient Raman bands of the S_1 state and discuss its molecular structure. Time-resolved vibrational spectra contain much information about the molecular structure of transient species even though it sometimes requires considerable effort to "read" spectra properly.[27−29] Especially, the vibrational frequency of a certain characteristic mode is very sensitive to the structural change taking place at the specific site of the molecule. Concerning the S_1 state of azobenzene, information about the structure around the central NN bond is the most important because it can afford a clue to understand how the S_1 state participates in the photoisomerization process. In this sense, the assignment of the NN stretching vibration is crucial. We synthesized a ^{15}N-substututed analogue and measured Raman spectra of the S_1 state in order to make an unambiguous assignment about this key vibration.

Figure 7 shows transient Raman spectra of the normal species and the ^{15}N analogue of the S_1 state of azobenzene. The spectra were measured for ethylene glycol solutions where the signal due to the vibrationally excited S_0 state was not observed. The Raman spectra of the S_0 state are also shown in this figure for comparison. In the S_0 spectra, the strongest Raman band at 1440 cm^{-1} exhibits a large ^{15}N shift of 29 cm^{-1}, which is accompanied by a small downshift of the neighboring band at 1471 cm^{-1}. This isotopic shift agrees with the literature[11] and ensures that the 1440 cm^{-1} band is assigned to the NN stretching vibration in the S_0 state. In the S_1 spectra, on the other hand, although the signal-to-noise ratio of the spectra was much worse than that of the S_0 spectra, it is clearly recognized that the Raman band at 1428 cm^{-1} shows a 27-cm^{-1} downshift with ^{15}N substitution. This S_1 band is straightforwardly attributable to the NN stretching vibration in the S_1 state. The ^{15}N shift of the S_1 band at 1428 cm^{-1} is almost the same as that of the NN stretch band in the S_0 spectrum (27 cm^{-1} in S_1 and 29 cm^{-1} in S_0). It implies that the corresponding vibrational modes in the S_1 and the S_0 state are very similar to each other and that there exists a fairly "pure" NN stretch mode in the S_1 state as well as in the S_0 state.

Vibrational assignments for the other S_1 Raman bands are safely made by referring to the vibrational assignments for the S_0 state,[11] because simple one-to-one correspondence can be made between the S_1 bands and the S_0 bands. The 1130 cm^{-1} band in the S_1 spectrum corresponds to the 1142 cm^{-1} band in the S_0 spectrum, and it is ascribed to the C−N stretch. The S_1

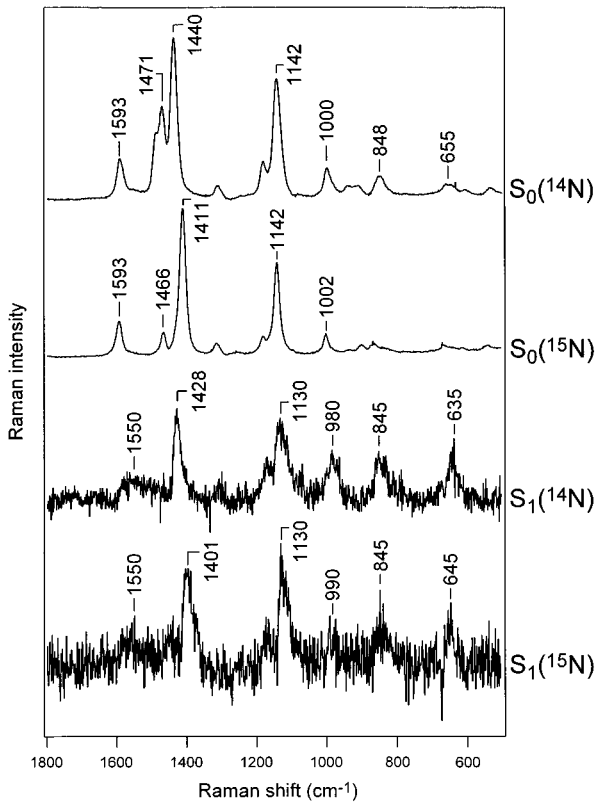

Figure 7. Raman spectra of *trans*-azobenzene in the S_1 state and in the S_0 state (in ethylene glycol): from the top to the bottom, normal species in the S_0 state, ^{15}N analogue in the S_0 state, normal species in the S_1 state, and ^{15}N analogue in the S_1 state. The S_1 spectra were taken at 0 ps.

TABLE 1: Observed Vibrational Frequencies and Their Assignments (in cm^{-1})[a]

S_1		S_0		
^{14}N	^{15}N	^{14}N	^{15}N	assgnts[b]
1550	1550	1593	1593	CC str of phenyl ring (8a/b)
1428	1401	1440	1411	NN str + (19a/b)
1130	1130	1142	1142	CN str + (13/9a)
980	990	1000	1002	trigonal (12) + breathing (1)
845	845	848		out-of-plane CH bend (10a)
635	645	655		ring deformation (6a)

[a] The values are observed in ethylene glycol solution. [b] Descriptions in parentheses are the Wilson notations.

Raman bands observed at 980, 845, and 635 cm^{-1} correspond to the S_0 bands at 1000, 848, and 655 cm^{-1}. They are assignable to the three phenyl ring modes, "trigonal + breathing",[27,30] out-of-plane CH bending, and ring deformation, respectively. The weak and broad feature recognized around 1550 cm^{-1} is presumably ascribable to the CC stretching vibration of the phenyl ring which gives rise to the 1593 cm^{-1} band in the S_0 spectrum. The vibrational frequencies observed in S_1 Raman spectra and their vibrational assingments are listed in Table 1 along with corresponding frequencies in the S_0 state.

The NN stretch frequency in the S_1 state (1428 cm^{-1}) that has been determined by ^{15}N substitution is slightly lower than the corresponding frequency in the S_0 state (1440 cm^{-1}), but the frequency difference is very small (12 cm^{-1}). This small change of the central NN stretching frequency indicates that the structural change induced by nπ* excitation is very small around the NN bond. The high NN stretching frequency in the S_1 state manifests that the NN bond in S_1 azobenzene retains a double bond character. In the S_1 state having nπ* character, an electron is excited from nonbonding n orbital to an antibonding π* orbital, which is expected to induce weakening of the relevant chemical bonds. The fact that only very small change is induced around the NN bond upon nπ* excitation suggests that π* orbital is not localized on the central NN bond, but it extends to the phenyl group. The vibrational frequencies of all observed phenyl ring modes shift downward by a few tens of wavenumbers in the S_1 spectrum. It also suggests the delocalization of the antibonding π* orbital over the whole molecule.

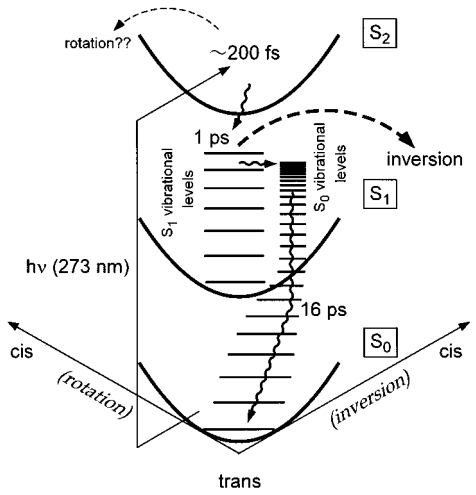

Figure 8. Schematic diagram of the relaxation process of *trans*-azobenzene in hexane after $S_2 \leftarrow S_0$ photoexcitation. See text.

The potential surface of the S_1 state should be different significantly from that of the S_0 state, and it causes the very fast trans $\rightarrow$ cis structural change in the S_1 state. One might expect a significant shift in equilibrium geometry along some coordinate in the S_1 state for the isomerization to happen. The present Raman data give clear evidence that this coordinate is not torsional, even if such a shift exists. The double bond nature of the NN bonding as well as high similarity in the spectral feature between S_1 Raman and S_0 Raman strongly suggests that the observed S_1 azobenzene has a planar structure around the central NN bond.

3.4. Relaxation Process of Photoexcited *trans*-Azobenzene. Figure 8 shows a sketch for the relaxation process of photoexcited azobenzene that was observed in the present study. The 273-nm light initially excites the molecule to the S_2 ($\pi\pi$*) state. This S_2 state is relaxed very rapidly (~200 fs) to generate the vibrationally excited S_1 (nπ*) state that exhibits a transient absorption around 400 nm. The present time-resolved Raman study revealed that the NN stretching frequency in the S_1 state is 1428 cm^{-1}, which is very close to that in the S_0 state (1440 cm^{-1}). This fact indicates that the NN bond in the S_1 state retains a double bond character, and hence, it suggests that the S_1 state has a planar structure around the NN bond. (Thus, we locate the potential minimum of the S_1 state roughly at the trans configuration in the figure.) Concerning the following $S_1 \rightarrow S_0$ relaxation, it was confirmed that the lifetime of the S_1 state significantly depends on the solvent. In hexane, the hot S_1 state is electronically relaxed to the S_0 state with a time constant as short as 1 ps to produce the vibrationally excited S_0 state. The appearance and the population change of the "hot" S_0 state were monitored in time-resolved Raman spectra in the anti-Stokes side. The S_0 state is cooled with a time constant of ~16 ps by dissipating its excess vibrational energy to the surrounding solvent. In ethylene glycol, on the other hand, the lifetime of the S_1 state becomes as long as 12.5 ps. Owing to the long S_1 lifetime, it is likely that significant amount of the energy is

dissipated to the surrounding solvent already in the S_1 state. Subsequently, the $S_1 \rightarrow S_0$ electronic relaxation takes place to give the vibrational excited S_0 state, which is cooled to reach thermal equilibrium. In the present Raman experiments for ethylene glycol solutions, the signal due to the vibrational excited S_0 state was hardly observed, indicating that only little population of the hot S_0 state appears during the relaxation process. This fact is readily rationalized in terms of the rate equation, which shows that the population of the hot S_0 state is determined by the balance between the $S_1 \rightarrow S_0$ relaxation rate (production of the hot S_0 state) and the vibrational cooling rate of the S_0 state (loss of the hot S_0 state). The $S_1 \rightarrow S_0$ relaxation rate observed in ethylene glycol is comparable to the vibrational cooling rate in hexane. In addition, if we take it account that a typical vibrational cooling rate in ethylene glycol is about double of that in hexane,[25] we can consider that the vibrational relaxation rate is significantly larger than the $S_1 \rightarrow S_0$ relaxation rate in ethylene glycol. This condition keeps the population of the hot S_0 state small and difficult to be observed because the rate of the loss is larger than the rate of the production.

Now we compare the conclusion obtained from the present picosecond time-resolved Raman study with the results of time-resolved UV−visible absorption spectroscopy reported by Lednev et al.[15−17] In the case of photoexcitation to the S_2 state, they found two components in the temporal change of absorption around 400 nm: the short-lived major component having a lifetime of ∼1 ps and the long-lived minor component with a lifetime of ∼15 ps. They interpreted this observation on the basis of the potential energy diagram calculated by Monti et al.[12] and assigned these two components to the "bottleneck" states in the S_2 and the S_1 potential. Especially, they suggested that "bottleneck" state in the S_1 potential has the 90° twisting configuration of a phenyl ring around the NN bond. The time constants of the dynamics observed in the present Raman study are in very good agreement with those of the two components found in the time-resolved absorption study. However, the assignments are different. Time-resolved Raman data clearly showed that the 1-ps dynamics is the decay of the S_1 state and the ∼16-ps dynamics (∼15 ps in the absorption study) is the vibrational cooling process in the S_0 state. Since our Raman probing wavelength is 410 nm and the observed time constants are very similar, it is highly likely that the dynamics observed in the Raman experiments are identical to those observed in the UV−visible absorption. Therefore, the present Raman study requests the revision of the former interpretation about the time-resolved absorption data.

The S_1 state observed in time-resolved measurements after $S_2 \leftarrow S_0$ photoexcitation is not the "twisted" bottleneck state that is expected to appear in the isomerization process of the rotation mechanism. It is not surprising because the lifetimes of the twisted intermediates of photoisomerization reactions are usually very short and it is very difficult to measure such transients by spectroscopic methods, even though there are a few exceptional molecules whose twisted states have fairly long lifetimes.[31−34] On reflection, it seems that there is no direct evidence indicating that the observed S_1 state participates in rotational mechanism of photoisomerization. The Raman spectra of the S_1 state strongly suggest that it has a planar structure around the NN bond and that its structure is not drastically changed from that of the S_0 state. It is likely that the relevant potential minimum in the S_1 state is rather closely located above the potential minimum of the S_0 state, even though some change in equilibrium geometry exists. The isomerization of the inversion mechanism has been considered to start from the S_1 state that is prepared by the direct $S_1 \leftarrow S_0$ photoexcitation,[4] which means that the inversion isomerization starts in the S_1 state just above the potential minimum of the S_0 state because the optical transition takes place vertically. Therefore, it seems that the planar S_1 state observed after $S_2 \leftarrow S_0$ photoexcitation is also the state from which the inversion mechanism starts, as indicated in Figure 8. One may deny this idea by mentioning that the lifetime of the S_1 state produced by the $S_2 \rightarrow S_1$ relaxation is different from that of the S_1 state prepared by direct $S_1 \leftarrow S_0$ photoexcitation. In hexane, the former value is ∼1 ps, but the latter one has been determined as 2.6 ps by time-resolved UV−visible absorption.[16] The lifetime is certainly one of the most important and characteristic property of the excited state, and in solution, it is usually insensitive to the photoexcitation wavelength. Thus it sounds fairly safe to refer to the lifetime for identifying the transient species that are produced by different pathways. However, we think, it is safe only when the lifetime of the transient is much longer than the time constant of vibrational cooling process because, in this case, what one measures is the lifetime of thermally equilibrated transient that has already dissipated its initial excess energy to the surrounding solvent. The situation is different for the transient species that decays much faster than vibrational cooling, since in this case we measure the lifetime of the transient species that still preserves its initial excess vibrational energy. Actually, in the gas phase where the vibrational cooling process takes place very slowly, the lifetime of the electronically excited state sometimes exhibits significant dependence on the vibrational energy.[35] Obviously, the lifetime of the S_1 azobenzene is much shorter than the vibrational cooling time in hexane. The lifetime of the S_1 state that we observed with the S_2 excitation is the lifetime of the highly vibrational excited state of the S_1 state. It may be different from the lifetime of the S_1 state created by direct $S_1 \leftarrow S_0$ photoexcitation reflecting the difference in the vibrational excess energy. To verify this argument, it is highly desirable to measure time-resolved Raman of the S_1 state that is created by direct $S_1 \leftarrow S_0$ photoexcitation. Unfortunately it is not easy task because the molar absorption coefficient of the $S_1 \leftarrow S_0$ absorption is small.

Finally, we make a comment on the rotational mechanism of photoisomerization of azobenzene. The rotational mechanism is the established mechanism for photoisomerization of olefins. For azobenzene, however, it seems that the existence of this isomerization pathway has not been fully proved whereas the inversion pathway was experimentally verified using chemical modification.[4−6] In fact, the present time-resolved Raman study did not give any support for the rotational mechanism but suggested that the inversion mechanism may take part also in the isomerization following the S_2 ($\pi\pi^*$) photoexcitation. To the authors' best knowledge, there has been no direct experimental evidence supporting the rotational pathway for isomerization of azobenzene. Also from the viewpoint of theoretical calculation, only little information is now available for azobenzene. The potential diagram, which we can refer to, was drawn on the basis of the ab initio MO calculations carried out only for several geometries using the minimum basis set.[12] Therefore, as for the rotational mechanism of azobenzene, we think that the existence itself should be reconsidered and is a subject for further theoretical and experimental investigation.

Acknowledgment. One of the authors (T.F.) is indebted to a Research Fellowship of the Japan Society for the Promotion of Science for Young Scientists. This work was partly supported

by the Grant-in Aids for Scientific Research (C) (No. 11640521) by the Ministry of Education, Science, Sports, and Culture of Japan.

References and Notes

(1) Liu, Z. F.; Hashimoto, K.; Fujishima, A. *Nature* **1990**, *347*, 658.
(2) Sekkat, Z.; Dumont, M. *Appl. Phys. B* **1992**, *54*, 486.
(3) Ikeda, T.; Tsutsumi, O. *Science* **1995**, *268*, 1873.
(4) Rau, H.; Lüddecke, E. *J. Am. Chem. Soc.* **1982**, *104*, 1616.
(5) Rau, H. *J. Photochem.* **1984**, *26*, 221.
(6) Rau, H.; Yu-Quan, S. *J. Photochem. Photobiol.* **1988**, *A42*, 321.
(7) Siampiringue, N.; Guyot, G.; Monti, S.; Bortolus, P. *J. Photochem.* **1987**, *37*, 185.
(8) Okamoto, H.; Hamaguchi, H.; Tasumi, M. *Chem. Phys. Lett.* **1986**, *130*, 185.
(9) Biswas, N.; Umapathy, S. *Chem. Phys. Lett.* **1995**, *236*, 24.
(10) Curtis, R. D.; Hilborn, J. W.; Wu, G.; Lumsden, M. D.; Wasylishen, R. E.; Pincock, J. A. *J. Phys. Chem.* **1993**, *97*, 1856.
(11) Armstrong, D. R.; Clarkson, J.; Smith, W. E. *J. Phys. Chem.* **1995**, *99*, 17825.
(12) Monti, S.; Orlandi, G.; Palmieri, P. *Chem. Phys.* **1982**, *71*, 87.
(13) Struve, W. S. *Chem. Phys. Lett.* **1977**, *46*, 15.
(14) Morgante, C. G.; Struve, W. S. *Chem. Phys. Lett.* **1979**, *68*, 267.
(15) Lednev, I. K.; Ye, T.-Q.; Hester, R. E.; Moore, J. N. *J. Phys. Chem.* **1996**, *100*, 13338.
(16) Lednev, I. K.; Ye, T.-Q.; Matousek, P.; Towrie, M.; Foggi, P.; Neuwahl, F. V. R.; Umapathy, S.; Hester, R. E.; Moore, J. N. *Chem. Phys. Lett.* **1998**, *290*, 68.
(17) Lednev, I. K.; Ye, T.-Q.; Abbott, L. C.; Hester, R. E.; Moor, J. N. *J. Phys. Chem. A* **1998**, *102*, 9161.
(18) Azuma, J.; Tamai, N.; Shishido, A.; Ikeda, T. *Chem. Phys. Lett.* **1998**, *288*, 77.
(19) Nägele, T.; Hoche, R.; Zinth, W.; Wachtveitl, J. C*hem. Phys. Lett.* 1**997**, *272*, 489.
(20) Hamm, P.; Ohline, S. M.; Zinth, W. L. *J. Chem. Phys.* **1997**, *106*, 519.
(21) Shimojima, A.; Tahara, T. Manuscript in preparation.
(22) Fieser, L. F.; Williamson, K. L. *Organic Experiments*, 4th ed.; Maruzen: Tokyo, 1980; Chapter 39.
(23) Asano, T.; Okada, T.; Shinkai, S.; Shigematsu, K.; Kusano, Y.; Manabe, O. *J. Am. Chem. Soc.* **1981**, *103*, 5161.
(24) Elsaesser, T.; Kaiser, W. *Annu. Rev. Phys. Chem.* **1991**, *42*, 83.
(25) Iwata, K.; Hamaguchi, H. *J. Phys. Chem. A* **1997**, *101*, 632.
(26) Sarkar, N.; Takeuchi, S.; Tahara, T. *J. Phys. Chem. A* **1999**, *103*, 4808.
(27) Tahara, T.; Hamaguchi, H.; Tasumi, M. *J. Phys. Chem.* **1987**, *91*, 5875.
(28) Tahara, T.; Hamaguchi, H.; Tasumi, M. *Chem. Phys. Lett.* **1988**, *152*, 135.
(29) Tahara, T.; Hamaguchi, H.; Tasumi, M. *J. Phys. Chem.* **1990**, *94*, 170.
(30) Tasumi, M.; Urano, T.; Nakata, M. *J. Mol. Struct.* **1986**, *146*, 383.
(31) Greene, B. I. *Chem. Phys. Lett.* **1981**, *79*, 51.
(32) Barbara, P. F.; Rand, S. D.; Rentzepis, P. M. *J. Am. Chem. Soc.* **1981**, *103*, 2156.
(33) Schilling, C. L.; Hilinski, E. F. *J. Am. Chem. Soc.* **1988**, *110*, 2296.
(34) Tahara, T.; Hamaguchi, H. *Chem. Phys. Lett.* **1994**, *217*, 369.
(35) Fleming, G. R. *Chemical Applications of Ultrafast Spectroscopy*; Oxford University Press: New York, 1986; Chapter 6.